ELSEVIER

Catalysis Today 81 (2003) 297–305

CATALYSIS TODAY

www.elsevier.com/locate/cattod

Peculiarities of ethane oxidation on V_2O_5/SiO_2 catalysts with different silica structure and morphology

A.V. Kucherov*, A.V. Ivanov, T.N. Kucherova, V.D. Nissenbaum, L.M. Kustov

Zelinsky Institute of Organic Chemistry, RAS, Leninsky Prosp. 47, 119991 Moscow, Russia

Abstract

Peculiarities of catalytic ethane oxidation with O_2 are studied on a series of V_2O_5/SiO_2 catalysts prepared by impregnation/oxidative calcination. Catalysts differ in structure and morphology of the starting silica. The samples supported on amorphous SiO_2 prepared by different methods (S_{BET} 330–680 m^2/g) are compared with catalysts supported on SiO_2 with mesoporous MCM-41 structure and silicalite with ZSM-5 structure. FTIR, DTA and ESR techniques are used to monitor the properties of catalysts. Catalytic testing at 450–600 °C demonstrates a drastic difference in the selectivity of the oxidation process on vanadia species stabilized by different types of silica. The catalyst supported on SiO_2 prepared by sol–gel method shows substantial activity in total ethane oxidation, with negligible contribution of oxidative dehydrogenation (ODH). On the other hand, the sample V_2O_5/MCM-41 demonstrates a surprisingly high level of ethene formation and relatively low activity in total oxidation, with selectivity of dehydrogenation reaching ~50% at 500–600 °C. Only trace amounts of oxygenates are formed in all cases. ESR data demonstrate a substantial difference in dispersion and redox properties of supported active V-phases in catalysts. Thus, peculiarities of the structure and morphology of the pure silica can control the structure and redox properties of the supported vanadium oxide species even in the absence of modifying additives.

Keywords: Ethane oxidation; Oxidative dehydrogenation; V_2O_5/SiO_2 catalysts; FTIR; ESR

1. Introduction

Vanadium oxide species are known to be active components of different composite catalysts for oxidative transformations of C_1–C_3 alkanes into oxygenates and olefins. At the same time, contradictary data were reported about the influence of the support, namely silica, on activity and selectivity of doped supported V_2O_5 catalysts [1–14].

The aim of our work is to monitor the catalytic behavior of the simplest binary systems, with active vanadium oxide species stabilized by different types of catalytically inert silica. Catalysts chosen, with approximately the same surface concentration of V_2O_5, differ substantially in structure and morphology of the starting silica.

2. Experimental

2.1. Catalyst preparation

In preparation of the series of disperse supported catalysts the question arises how to provide better conditions for comparative study. Samples with the identical weight concentration of the active phase, V_2O_5, are less acceptabe, in our opinion, in the case of silica with substantially different surface areas (330–1100 m^2/g). Our choice is to provide approximately an equal

---

* Corresponding author.
E-mail address: avk@ioc.ac.ru (A.V. Kucherov).

0920-5861/03/$ – see front matter © 2003 Elsevier Science B.V. All rights reserved.
doi:10.1016/S0920-5861(03)00121-4

surface concentrations of V ions on the SiO_2 samples, namely ~1 μmol V per 1 m^2 of silica. The coverage is much lower than a monolayer, $\sim 5 \times 10^{18}$ molecules of V_2O_5 per 1 m^2 being considered as the amount necessary to form a monolayer on a support.

The method of MCM-41 preparation was given in [15] and it was similar to the method described elsewhere [16]. The sample 9.1 wt.%.V_2O_5/MCM-41 was prepared by impregnation of MCM-41 ($S_{BET} = 1100\,m^2/g$) with an aqueous solution of NH_4VO_3 followed by drying at room temperature overnight. The amount of the added component was selected as 1 mmol (51 mg) of V per 1 g of MCM-41. The sample was then calcined at 540 °C in a flow of air for 18 h. X-ray diffraction patterns of MCM-41 confirm the preservation of a structure typical of the mesoporous MCM-41 molecular sieve.[1]

Amorphous thermostable SiO_2 with $S_{BET} = 680\,m^2/g$ was prepared from tetraethoxysilane using cellulose templating approach [17] with subsequent burning off of the organic template in an air flow at ~600 °C. Then the sample 6 wt.% $V_2O_5/(SiO_2)_{burn}$ was prepared by a three-fold incipient wetness impregnation of this silica with an aqueous NH_4VO_3 solution of the specified concentration with subsequent calcination of the catalyst at 500 °C for 2 h on air.

The original sample of the industrial aerosil SiO_2 (KSK) contained a considerable admixture of iron oxides. Therefore, this support was treated with a 5% aqueous HCl solution to remove the main part of the iron impurities. Silica (10 g; fraction 0.5–1 mm) was added to ~200 cm^3 of the HCl solution, kept overnight, heated to 60 °C for 30 min, and washed out with distilled water. Treatment was repeated five times. Dried purified silica, with $S_{BET} = 310\,m^2/g$, was used for preparation of the catalyst 3 wt.% $V_2O_5/(SiO_2)_{KSK}$. The sample was prepared by a five-fold incipient wetness impregnation/drying of the silica using an aqueous NH_4VO_3 solution of the specified concentration, with a final calcination of the catalyst at 500 °C for 2 h on air. The Pd-doped sample was also prepared by impregnation of this catalyst by a solution of $PdCl_2$ with subsequent oxidative calcination at 500 °C. The palladium content was 0.07 wt.% which corresponded to the atomic ratio Pd/V ~1/50.

The sample of SiO_2 was prepared using a tetraethoxysilane solution by a conventional sol–gel method. Hydrolysis of a homogeneous ethanolic solution at room temperature was initiated by diluted aqueous HNO_3, and the glass-like sample obtained after 24–48 h was dried in an air flow and calcined at 500 °C for 5 h. This amorphous silica ($S_{BET} = 330\,m^2/g$ after oxidative calcination) was impregnated with an aqueous NH_4VO_3 solution and dried on air. Treatment was repeated five times, and finally the sample 3 wt.% $V_2O_5/(SiO_2)_{sol-gel}$ was calcined in an air flow at 500 °C for 2 h.

The sample of silicalite with a low Al content ($SiO_2/Al_2O_3 = 420$, crystallinity ~90%; PQ Corp.) was used for preparation of the catalyst 3 wt.% V_2O_5/silicalite by a five-fold incipient wetness impregnation of the support with an aqueous NH_4VO_3 solution of the specified concentration with final calcination of the catalyst at 500 °C for 4 h on air. The reference sample 3 wt.% V_2O_5/HZSM-5 was prepared by the same method using H-ZSM-5 zeolite ($SiO_2/Al_2O_3 = 50$, crystallinity ~95%; PQ Corp.) as a support.

Since the introduced amount of vanadium was retained by the impregnated samples, no further analysis was done.

2.2. Catalytic testing

The catalysts were tested in ethane oxidation [18] at 400–600 °C by placing the sample (0.3–1.0 g; fraction 0.25–0.5 mm) to fill a ~1 cm^3 volume in a fixed-bed quartz reactor. The fresh catalyst loading was conditioned at 520 °C in a dry air flow (50 cm^3/min) for 2 h. Then the temperature of the catalytic run was fixed and the oxidant-deficient reaction mixture, $O_2/C_2H_6 = 1/2$, [4.04 vol.% C_2H_6 +2.06 vol.% O_2 + He] was fed to the reactor under 1 atm pressure and a space velocity of ~2400 h^{-1}. Catalyst activities were measured with accuracy ±10% at the ethane conversion from 1 to ~35% for the above-mentioned mixture of reactants. Samples of the reactor effluent were injected periodically into a chromatograph equipped with the Poropac-Q column and a catarometer.

For better identification of oxygenates formed at a given temperature, the reactor effluent was switched to the trap cooled by liquid N_2, and products

---

[1] Authors thank Dr. A. Shigapov (Scientific Research Lab., Ford Motor Co., Aahen) for synthesis of the sample.

accumulated after 1–2 h on stream were analyzed chromatographically.

After the catalytic testing, the catalyst sample was calcined *in situ* in the reaction mixture at 600 °C for 1 h and in an air flow at 750 °C for 2 h. Then the catalytic tests at 450–600 °C were repeated.

2.3. IR spectroscopic studies

IR spectra of SiO_2 supports were recorded at 20 °C in the diffuse reflectance mode ($8\,cm^{-1}$ resolution) using a Nicolet Protege 460 FTIR spectrometer. The crushed samples (fraction 0.2–0.5 mm) were placed in a quartz cell with a CaF_2 window, activated in O_2 (100 Torr) at 500 °C, and evacuated. The acidic sites were studied using CO and C_6D_6 as molecular probes. The Kubelka–Munk equation was used for the treatment of the spectra (OMNIC program).

2.4. DTA measurements

Combined TG–DTG–DTA analysis was done on "Derivatograph-C" (MOM Co.) under static conditions on air with a linear heating program (10°/min) up to 900 °C. Starting pure supports, fresh catalysts and samples after catalytic testing were studied.

2.5. ESR measurements

The ESR spectra were taken in the X-band ($\lambda \cong 3.2$ cm) at 20 °C on a Bruker ESP300 spectrometer equipped with a 4104OR cavity. The ESR signals were registered at a microwave power of 6.35 mW and modulation amplitude of 2.0 G in the field range of 2600–4200 G (5 scans with a sweep time of 42 s). The Bruker ESP300E software and the special Bruker program WIN-EPR (version 901201) were used for data processing.

Fresh catalysts were crushed into 0.1–0.2 mm particles, charges of the sample (30 ± 1 mg) were placed in identical quartz ampoules (3.5 mm diameter), calcined in a furnace at 500 °C for 10–15 min, connected to the vacuum system, evacuated for ~1 min to 0.03 Torr at 500 °C, and sealed off. Catalysts taken after catalytic testing were placed in the same quartz ampoules, connected to the vacuum system, evacuated for ~15 min to 0.03 Torr at room temperature, and sealed off. ESR spectra were registered at 20 °C and normalized for the differences in the sample weight. Then ampoules were open to air and ESR measurements were repeated. For the sake of accuracy, series of samples were measured consecutively, with ampoules in the same position inside the ESR resonator.

3. Results and discussion

The catalytic activity of crushed fused quartz (fraction 0.25–0.5 mm) was measured for evaluation of the contribution of homogeneous gas-phase reactions. Conversion of ethane was negligible (<4%) up to 600 °C, with formation of trace amounts of CO_2 and C_2H_4 at $T > 500$ °C. Pure $(SiO_2)_{sol–gel}$ taken as a reference demonstrated a higher ethane conversion: the CO_2 and CO yields reached ~6–8% at 560–600 °C, with a trace admixture of C_2H_4 (≤2%). It was noted earlier [19] that placing different solids into the reactor leads to a drastic change in reaction parameters of homogeneous reactions depending on the chemical nature of solids. Thus, in our testing conditions, the reactor filled with pure silica with a high surface area shows low but measurable oxidation activity.

The conversion of ethane into different products on the sample$V_2O_5/(SiO_2)_{sol–gel}$ calcined at 500 and 600 °C is presented in Fig. 1a and b, respectively, as a function of the reaction temperature. As compared with the pure support, the sample with the supported V-phase demonstrates a much higher oxidation rate, especially at T ~450–500 °C. Carbon dioxide is the main reaction product at any temperature, with yields reaching ~12–13% at 480–500 °C (Fig. 1a). As compared with a stoichiometric limit of CO_2 formation in our reaction mixture (~15%), this value points to a high rate of total oxidation on the catalyst active sites. The amount of C_2H_4 formed (Fig. 1b) does not exceed what detected for pure silica. Thus, vanadium oxide species stabilized by SiO_2 prepared by sol–gel method show substantial activity in total ethane oxidation to CO_2, with zero contribution of oxidative dehydrogenation (ODH).

Fig. 2 shows the conversion of ethane into different products on the samples V_2O_5/MCM-41 calcined at 600 and 750 °C. The samples demonstrate low conversion of ethane to CO_2 (reaching 5–6% at 600 °C) with a simultaneous high level of C_2H_4 and CO formation.

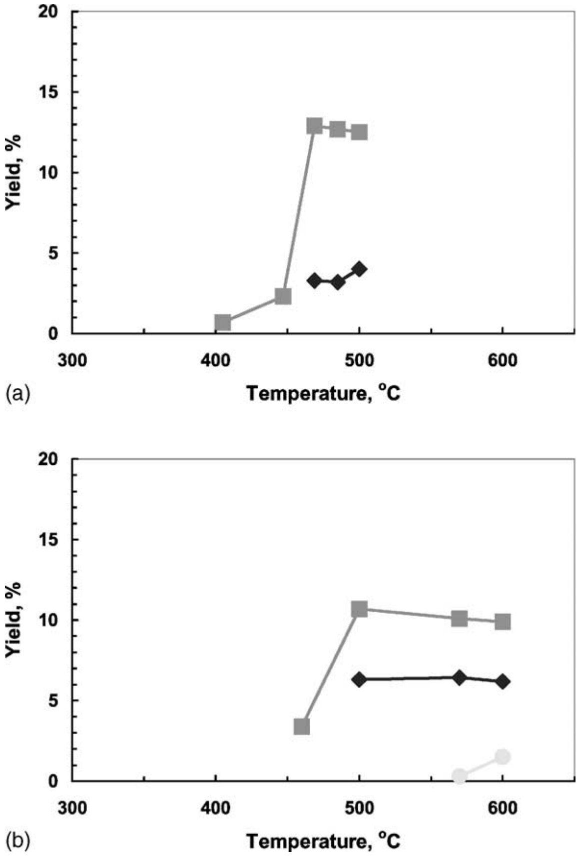

Fig. 1. Yield of ethene (●), CO (◆) and CO_2 (■) as a function of temperature for ethane oxidation on 3%$V_2O_5/(SiO_2)_{sol-gel}$ calcined at 500 °C (a) and 600 °C (b).

The selectivity of ethene formation, S_{ethene}, calculated as the ratio C_2H_4 formed/C_2H_6 converted, reaches 45–50% at $T \sim 550$–600 °C. Therefore, vanadium oxide species stabilized by silica-MCM-41 are quite active in ODH, with relatively low contribution of the total oxidation. This sample is also characterized by surprisingly high thermal stability: oxidative calcination at 750 °C for 2 h does not cause any loss of the catalyst activity and selectivity.

The conversion of ethane into different products on the sample$V_2O_5/(SiO_2)_{burn}$ calcined at 600 and 750 °C is presented in Fig. 3a and b. The catalyst demonstrates activity in both oxidation to CO and CO_2, as well as in ODH. Oxidative calcination of this specimen at 750 °C causes a moderate decrease in the catalyst activity and selectivity of ODH (from ∼40 to 30%).

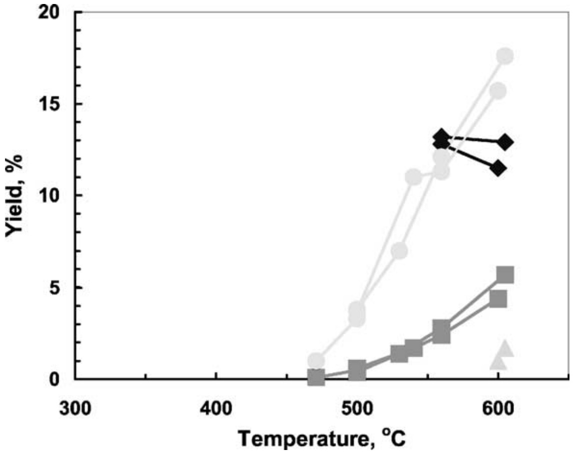

Fig. 2. Yield of ethene (●), CO (◆), CH_4 (▲) and CO_2 (■) as a function of temperature for ethane oxidation on 9%V_2O_5/MCM-41 calcined at 600 and 750 °C.

The yield of different products formed upon ethane oxidation on V_2O_5/silicalite is shown in Fig. 4a and b. Carbon dioxide is the main product, with S_{ethene} reaching ∼35% at $T > 500$ °C. Catalyst calcination at 750 °C does not change noticeably its activity and ODH selectivity (Fig. 4). The reference sample V_2O_5/HZSM-5 shows a similar temperature dependence of product distribution (Fig. 4), with a slightly higher level of CO formation and a lower yield of ethene ($S_{ethene} \sim 25\%$).

The yield of ethene upon C_2H_6 ODH on the sample$V_2O_5/(SiO_2)_{KSK}$ calcined at 500 °C reaches 6.4%, with $S_{ethene} \sim 50\%$. However, calcination of the sample at higher temperatures is accompanied by a sharp loss of activity and selectivity. The conversion of ethane into different products on the sample$V_2O_5/(SiO_2)_{KSK}$ calcined at 600 and 750 °C is presented in Fig. 5a and b, respectively. Thus, the surface of aerosil can, in principle, accomodate active V-species with catalytic properties similar to those found for V_2O_5/MCM-41, but this type of catalytic species in $V_2O_5/(SiO_2)_{KSK}$ is much less thermally stable.

Fig. 6 shows the same temperature dependence of the product formation for the reference doped sample $(Pd + V_2O_5)/(SiO_2)_{KSK}$. We expected that a small amount of Pd added ($V/Pd = 50$) will ensure deeper reduction of the supported vanadia phase without considerable contribution of Pd-species in catalysis. As one can see, introduction of just 0.07 wt.% Pd results

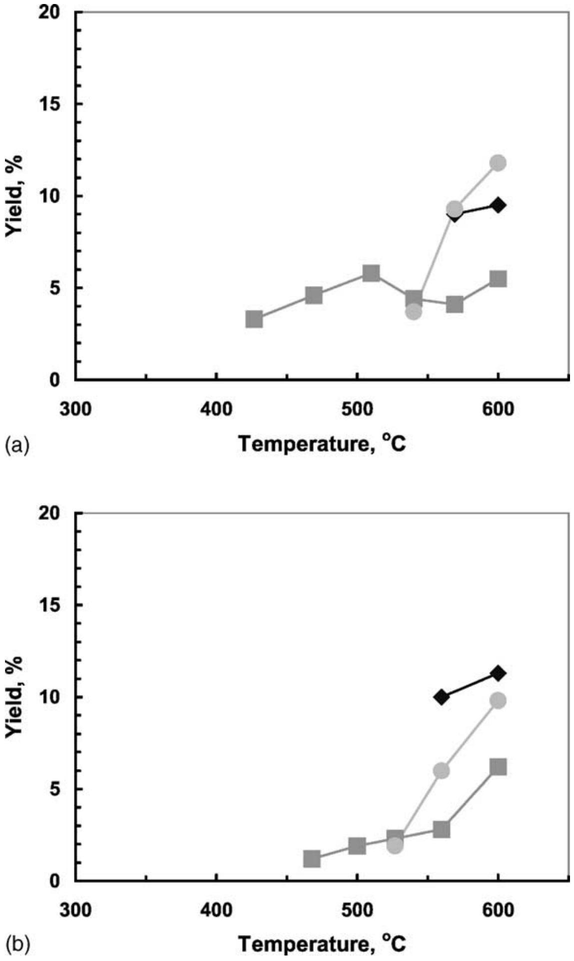

Fig. 3. Yield of ethene (●), CO (◆) and CO$_2$ (■) as a function of temperature for ethane oxidation on 6%V$_2$O$_5$/(SiO$_2$)$_{burn}$ calcined at 600 °C (a) and 750 °C (b).

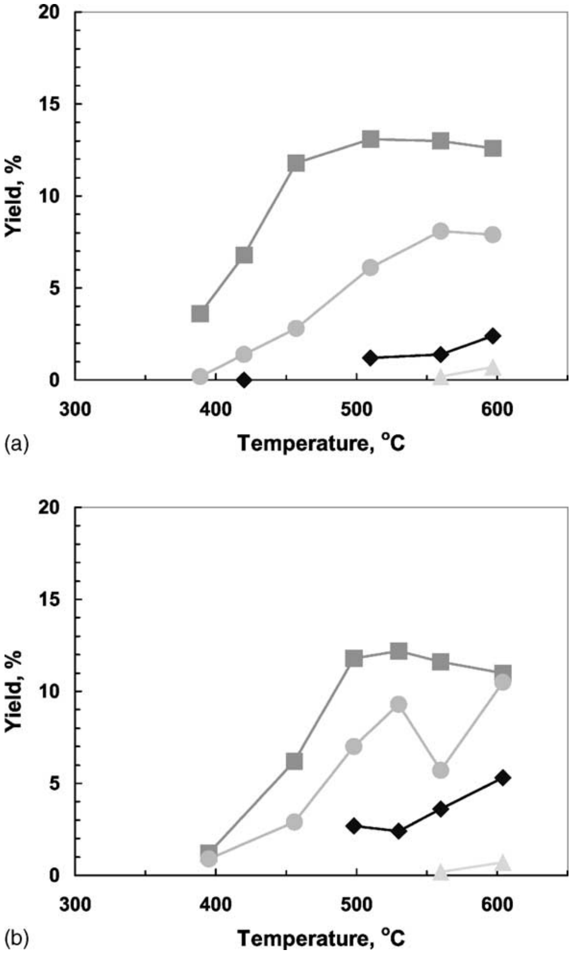

Fig. 4. Yield of ethene (●), CO (◆), CH$_4$ (▲) and CO$_2$ (■) as a function of temperature for ethane oxidation on 3%V$_2$O$_5$/silicalite calcined at 600 °C (a) and 750 °C (b).

in a dramatic change both in catalyst activity and selectivity (Figs. 5 and 6). No enhancement of ODH occurs as a result of Pd introduction, but the ethene yield is still considerable ($S_{ethene} \sim$ 25–30% at 600 °C). At the same time, the catalyst shows very high activity in total oxidation at lower temperatures. The CO$_2$ yield approaches 15% at 400 °C (Fig. 6) which is a stoichiometric limit for our reaction mixture. The question arises about the forms of oxygen-containing species involved in the chain of transformations leading to formation of CO and C$_2$H$_4$ at higher temperatures. Future studies of (CO$_2$ + C$_2$H$_6$) reaction could clarify this problem.

Summarizing the catalytic data obtained (Figs. 1–6), we conclude that, in all cases, CO, CO$_2$ and C$_2$H$_4$ are the main reaction products, with negligible formation of oxygenates and CH$_4$ at $T \leq 600$ °C. It may be related to relatively high vanadia loading in our samples: noticeable formation of oxygenates was detected earlier for a very low-loaded catalysts only [3,20,21] or for composite multicomponent systems [2,12,13,22–25]. Anyway, one can see a drastic difference in selectivity of the ethane total oxidation and ODH process on vanadium oxide species stabilized by different types of silica. In turn, it can be related only to a substantial difference in the dispersion

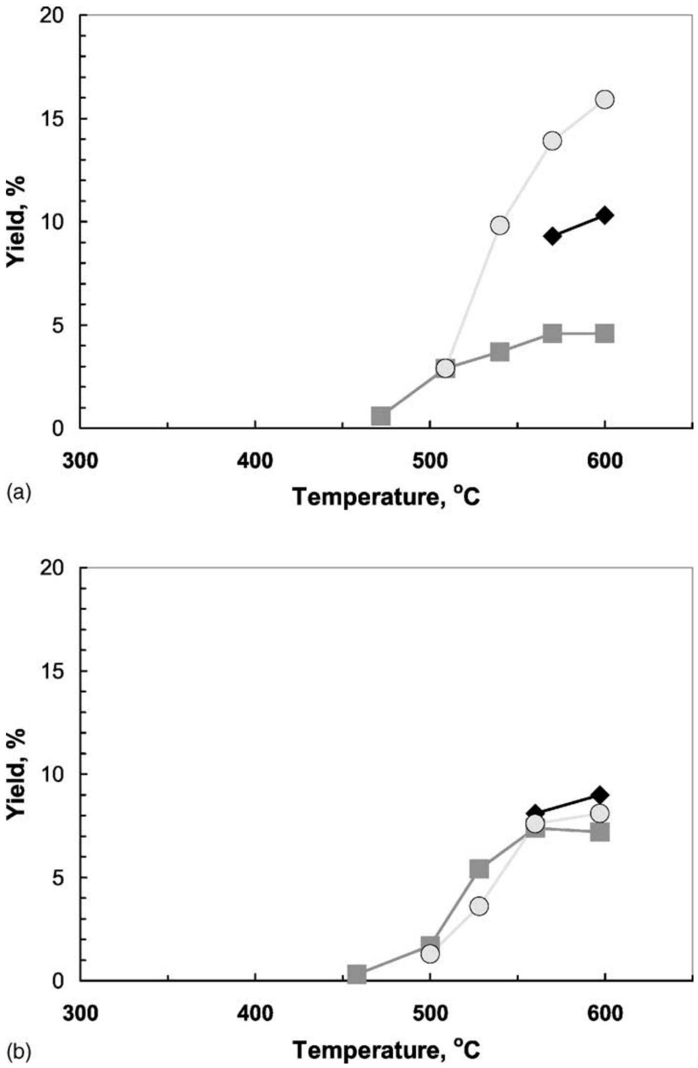

Fig. 5. Yield of ethene (○), CO (◆) and CO_2 (■) as a function of temperature for ethane oxidation on $3\%V_2O_5/(SiO_2)_{KSK}$ calcined at 600 °C (a) and 750 °C (b).

and redox properties of supported active V-phases in the catalysts. The properties of the supports and catalysts were studied using DTA, FTIR and ESR methods.

DTA analysis of starting pure supports shows that SiO_2 samples differ substantially in the water loss in the low-temperature region: $(SiO_2)_{sol-gel} > (SiO_2)_{KSK} > (SiO_2)_{burn} \sim$ MCM-41 $\sim$ silicalite. Introduction of vanadia leads to a substantial decrease in the water loss by catalysts confirming noticeable modification of the support surfaces by V_2O_5. No effect caused by burning off of carbonaceous deposits is detected for all the samples after catalytic testing. High-temperature effects caused by vanadia phase transformations are not characteristic.

Fig. 7 shows IR spectra of starting silica supports in the region of stretching and combination vibrations of –OH and SiOH groups. The simplest spectral picture is obtained for MCM-41 being typical of dehydroxylated SiO_2. The intense band at 3735–3740 cm^{-1} (Fig. 7)

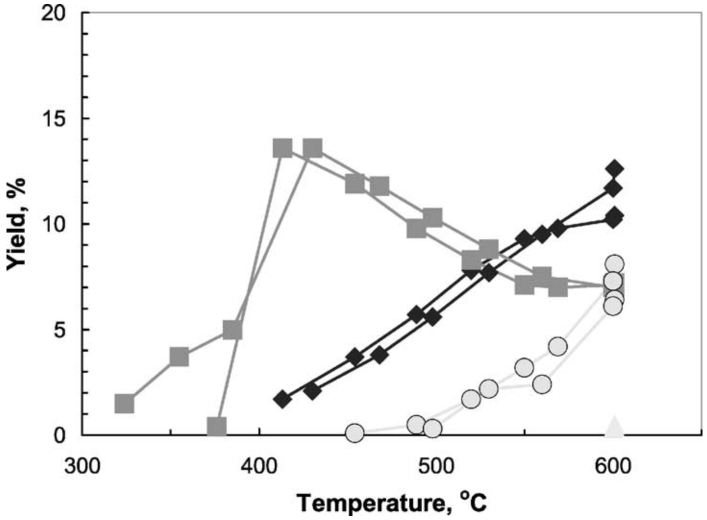

Fig. 6. Yield of ethene (●), CO (◆), CH$_4$ (▲) and CO$_2$ (■) as a function of temperature for ethane oxidation on (0.07%Pd + 3%V$_2$O$_5$)/(SiO$_2$)$_{KSK}$ calcined at 600 and 750 °C.

corresponds to the stretching vibrations of silanol OH groups [26]. A low-frequency shoulder at ~3600 cm^{-1} can be attributed to OH-groups forming H-bonds with either neighboring hydroxyls or lattice oxygens. Weak bands at 4530 and 4550 cm^{-1} can be attributed to the combination of stretching and in-plane bending vibrations of OH groups and combination of the stretching vibrations in O–H and Si–O bonds, respectively [27]. The intensity of the broad band at 3550 cm^{-1} typical of all OH groups forming H-bonding with neighboring hydroxyls increases in the spectrum of the (SiO$_2$)$_{KSK}$. However, the most pronounced increase of the intensity of the band of combination vibrations takes place for the system (SiO$_2$)$_{sol–gel}$. Therefore,

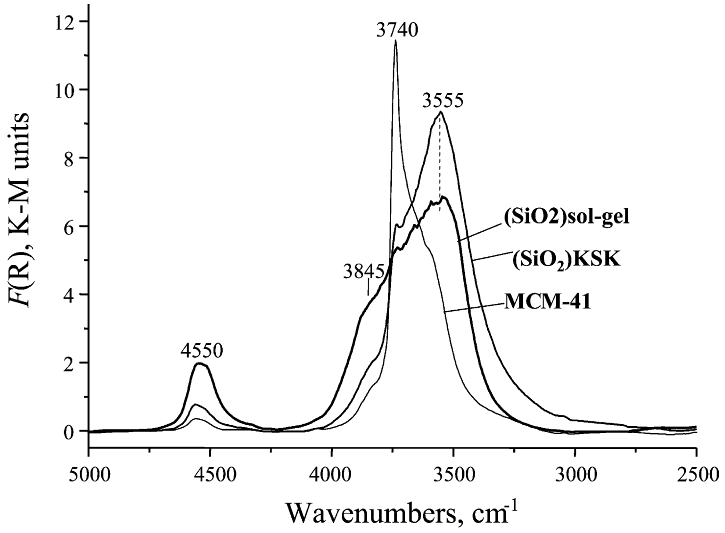

Fig. 7. FTIR spectra of OH groups of different silica samples.

this silica shows the highest extent of the surface hydroxylation.

In accordance with the literature data, adsorption of CO on pure silica samples is not accompanied by the appearance of bands from adsorbed CO. Thus, pure starting supports contain no Lewis acid sites. Benzene-d_6 sorption was used for characterization of Broensted acid sites (BAS). The shift of OH groups vibration band due to formation of hydrogen bonding can be taken as a measure of the BAS strength. The value of $\Delta\nu$OH is ~120 cm^{-1} for SiO_2–MCM-41 and $(SiO_2)_{sol–gel}$ samples which is close to the published data [28], and for the sample $(SiO_2)_{KSK}$ two maxima of the shifted bands are observed, with $\Delta\nu$OH ~150 and 95 cm^{-1}, respectively. Therefore, Broensted acidity of all silica samples is comparable.

Fresh catalysts calcined in air show no ESR signal from V^{4+} paramagnetic species except for the V_2O_5/silicalite sample demonstrating a weak signal with hfs typical of isolated V^{4+} ions in cationic positions created by residual Al^{3+} of the zeolitic lattice ($SiO_2/Al_2O_3 = 420$). A much stronger signal of the same type is observed for the V_2O_5/HZSM-5 reference sample ($SiO_2/Al_2O_3 = 50$). However, it was shown earlier that this specific type of vanadyl cations stabilized in ZSM-5 channels cannot be oxidized [29,30], so it is hard to imagine its participation in redox processes. Anyway, the number of these cations in silicalite is negligible, so that all vanadia in fresh catalysts forms the non-paramagnetic V^{5+} species.

ESR signals from the samples taken from the reactor after catalytic testing are presented in Fig. 8. This measurement permits us to compare the catalysts treated under identical conditions with the reaction mixture and reached a steady state in redox conditions of catalysis. No narrow lines typical of carbonaceous deposits is detected for all used catalysts in agreement with the above-mentioned DTA data. All catalysts are characterized by quite strong ESR signals from paramagnetic V^{4+}-containing phases. An intense rather narrow ESR singlet ($\Delta H \cong 170$ G; $g = 1.98$) with hfs traces is typical of V_2O_5/MCM-41 (Fig. 8a). The V_2O_5/silicalite sample shows a weak signal with well resolved hfs superimposed on a very broad line (Fig. 8b). The signal with hfs is identical to the signal from cations in channels seen in a fresh V_2O_5/silicalite, as mentioned above. So, the new signal formed after catalysis is the broad line with $\Delta H \cong$ 900 G and g-factor ~2.0. The $V_2O_5/(SiO_2)_{KSK}$ sample reduced under catalysis conditions demonstrates a symmetric singlet with ΔH = 200–210 G and $g \cong 1.99$ (Fig. 8c). The $V_2O_5/(SiO_2)_{sol–gel}$ system shows a very weak broad line only.

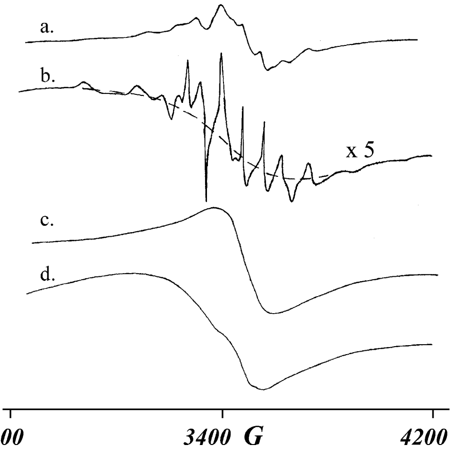

Fig. 8. ESR spectra, taken at 20 °C, of evacuated samples after catalytic testing. (a) 9%V_2O_5/MCM-41, (b) 3%V_2O_5/silicalite, (c) 3%$V_2O_5/(SiO_2)_{KSK}$, (d) (0.07%Pd + 3%V_2O_5)/$(SiO_2)_{KSK}$.

In general, ESR signals with hfs point to the presence of isolated V^{4+} ions whereas ESR-singlets without hfs are typical of magnetically interacting V^{4+} ions. The broader is the singlet, the larger is a cluster of ions containing V^{4+}-species. Accordingly, the MCM-41 matrix stabilizes the most disperse paramagnetic species of the active catalyst phase. However, contribution of isolated ions is small and the active phase contains small aggregated species. On the contrary, the $(SiO_2)_{sol–gel}$ surface stabilizes large vanadia species with a lower reduction degree. Easy aggregation in this case can be related to the peculiarities of the surface morphology only. Large V-species are also formed on the silicalite surface but it can be easily explained by taking into account a bi-disperse nature of this support. The total surface area of this sample, with narrow ZSM-5 channels, is ~600 m^2/g but the external surface of crystallits reaches 20–30 m^2/g only. If V-species are located on the outer surface mainly, the surface vanadia concentration in this sample is ~10 times higher than in other samples. Industrial aerosil (KSK) is able to stabilize rather small vanadyl-containing aggregates but this support demonstrates much lower thermal stability, as compared with MCM-41. ESR data confirm that addition of Pd promotes very substantially the reduction of the active phase: the broader asymmetric ESR signal from Pd + $V_2O_5/(SiO_2)_{KSK}$ ($\Delta H \cong 460\,G$) is much more intense as compared with the signal for $V_2O_5/(SiO_2)_{KSK}$ (Fig. 8c and d).

4. Conclusions

1. Catalytic testing at 450–600 °C demonstrates a substantial difference in selectivity of the oxidation process on vanadium oxide species stabilized by different types of silica. The catalyst supported on $(SiO_2)_{sol\text{–}gel}$ shows activity in total ethane oxidation, with negligible contribution of ODH. On the other hand, the sample V_2O_5/MCM-41 demonstrates a high level of ethene formation, with the selectivity of ethane ODH reaching ∼50%.
2. Catalysts show a substantial difference in thermal stability depending on the type of silica used. The sample $V_2O_5/(SiO_2)_{KSK}$ loses the starting high activity and selectivity in ethene formation after oxidative calcination at 750 °C, whereas the catalyst V_2O_5/MCM-41 remains intact after the same treatment.
3. Only trace amounts of oxygenates are formed on all binary V_2O_5/SiO_2 catalysts.
4. No deposition of "coke" occurs upon catalytic testing of V_2O_5/SiO_2 samples.
5. Peculiarities of V_2O_5/SiO_2 catalytic properties can be related to a substantial difference in dispersion and redox properties of supported active V-phases in the catalysts. Thus, the structure and morphology of pure silica can control the structure and redox properties of the supported vanadium oxide species.

References

[1] M.A. Banares, X.T. Gao, L.G. Fierro, I.E. Wachs, Stud. Surf. Sci. Catal. 110 (1997) 295.
[2] M. Merzouki, B. Taouk, L. Tessier, E. Bordes, P. Courtine, Stud. Surf. Sci. Catal. 75 (1993) 753.
[3] Z. Zhao, Y. Yamada, Y.H. Teng, A. Ueda, K. Nakagawa, T. Kobayashi, J. Catal. 190 (2000) 215.
[4] J. Lebars, A. Auroux, J.C. Vedrine, M. Baerns, Stud. Surf. Sci. Catal. 72 (1992) 181.
[5] X.T. Gao, M.A. Banares, I.E. Wachs, J. Catal. 188 (1999) 325.
[6] T. Blasco, A. Galli, J.M.L. Nieto, F. Trifiro, J. Catal. 169 (1997) 203.
[7] J. Lebars, A. Auroux, M. Forissier, J.C. Vedrine, J. Catal. 162 (1996) 250.
[8] V.P. Vislovskiy, V.Y. Bychkov, M.Y. Sinev, N.T. Shamilov, P. Ruiz, Z. Schay, Catal. Today 61 (2000) 325.
[9] A. Erdohelyi, F. Solymosi, J. Catal. 123 (1990) 31.
[10] Z.Y. Dang, J.F. Gu, J.Z. Lin, D.X. Yang, Catal. Lett. 54 (1998) 129.
[11] A. Galli, J.M.L. Nieto, A. Dejoz, M.I. Vazquez, Catal. Lett. 34 (1995) 51.
[12] L. Tessier, E. Bordes, M. Gubelmann-Bonneau, Catal. Today 24 (1995) 335.
[13] A. Erdohelyi, F. Solymosi, Appl. Catal. 39 (1988) L11.
[14] J. Lebars, J.C. Vedrine, A. Auroux, S. Trautmann, M. Baerns, Appl. Catal. A: Gen. 88 (1992) 179.
[15] A.V. Kucherov, A.V. Ivanov, T.N. Kucherova, A.N. Shigapov, Microporus Mesoporus Mater., submitted for publication.
[16] G. Grubert, J. Rathousky, G. Schulz-Ekloff, M. Wark, A. Zukal, Microporous Mesoporous Mater. 22 (1998) 225.
[17] A.N. Shigapov, G.W. Graham, R.W. McCabe, H.K. Plummer, Appl. Catal. A: Gen. 210 (2001) 287.
[18] A.V. Kucherov, T.N. Kucherova, A.A. Slinkin, Catal. Lett. 10 (1991) 289.
[19] V.P. Vislovskiy, T.E. Suleimanov, M.Yu. Sinev, Yu.P. Tulenin, L.Ya. Margolis, V. Cortes Corberan, Catal. Today 61 (2000) 287.
[20] Y. Yamada, Z. Zhao, A. Ueda, T. Kobayashi, in: Proceedings of the NATO Advance Reservoir Workshop of Catalysis by Unique Metal Ion Structures in Solid Matrices, Prague, 4–7 July 2000, p. 28.
[21] Z. Zhao, Y. Yamada, A. Ueda, H. Sakurai, T. Kobayashi, Appl. Catal. A: Gen. 196 (2000) 37.
[22] M. Merzouki, B. Taouk, L. Monceaux, E. Bordes, P. Courtine, Stud. Surf. Sci. Catal. 72 (1992) 165.
[23] K. Ruth, R. Burch, R. Kieffer, J. Catal. 175 (1998) 27.
[24] N.F. Chen, K. Oshihara, W. Ueda, Catal. Today 64 (2001) 121.
[25] M. Roy, M. Gubelmann-Bonneau, H. Ponceblanc, J.C. Volta, Catal. Lett. 42 (1996) 93.
[26] L.H. Little, Infrared Spectra of Adsorbed Species, Academic Press, London, New York, 1966.
[27] L.M. Kustov, V.Yu. Borovkov, V.B. Kazanskii, Zh. Fiz. Khim. Russ., J. Phys. Chem. 59 (1985) 2213.
[28] V.B. Kazansky, L.M. Kustov, V.Yu. Borovkov, Zeolites 3 (1983) 77.
[29] A.V. Kucherov, A.A. Slinkin, Zeolites 7 (1987) 43.
[30] A.V. Kucherov, A.A. Slinkin, Zeolites 7 (1987) 583.